Green Chemistry

PAPER

View Article Online
View Journal | View Issue

Cite this: *Green Chem.*, 2024, **26**, 9869

Highly efficient electrosynthesis of oximes from nitrates and carbonyl compounds in acidic media†

Cheng Xue,[a,b] Shuaiqiang Jia,*[a,b] Jiapeng Jiao,[a,b] Xiao Chen,[a,b] Zhanghui Xia,[a,b] Mengke Dong,[a,b] Ting Deng,[a,b] Hailian Cheng,[a,b] Chunjun Chen,[a,b] Haihong Wu,*[a,b] Mingyuan He[a,b] and Buxing Han*[a,b,c]

Received 13th July 2024,
Accepted 25th August 2024

DOI: 10.1039/d4gc03429e

rsc.li/greenchem

Electrocatalytic nitrate reduction reaction (NO_3RR) coupled with organic compounds to synthesize oximes for value-added conversion of waste pollutants has very promising prospects. However, due to the susceptibility of the feedstock to hydrogenation, the relatively low reaction efficiency, and the poor stability of oximes, the reaction in acidic electrolytes remains a formidable challenge. Herein, we report a novel strategy for the one-step synthesis of oximes from nitrite and aldehydes/ketones in acidic electrolytes using a Zn-based catalyst (multilayered Zn nanosheet catalyst, M-ZnNSs). 99% yield and 99% selectivity of phenylacetaldehyde oxime were achieved at a constant current of –12 mA cm^{-2}. Moreover, various aldehydes/ketones were efficiently converted to oximes with yield and selectivity up to >90%, demonstrating the high versatility of this method. Furthermore, the catalyst exhibited remarkable long-term stability (>100 h). This work proposes a green strategy to promote the recycling of nitrogen resources, enhance the value of NO_3^- conversion products, and develop new ideas for electrochemical C–N coupling.

Introduction

Anthropogenic emissions of nitrogen oxides (NO_x) have increased rapidly over the past century, posing a threat to human health and ecosystems.[1,2] Various methods have been employed to remove NO_x.[3–5] Among them, electrocatalysis has received much attention from researchers due to its environmental friendliness, energy saving, simple operation and controllable products.[6,7] Most of the studies on electrocatalytic nitrate reduction reactions are based on the *in-situ* generation of NH_2OH for the preparation of C–N coupling products in tandem with other suitable reactions to transform waste pollutants into high value-added chemicals.[8–16] Oximes are important intermediates in organic synthesis and have proved to be industrially useful as fine chemicals.[17–19] For instance, cyclohexanone oxime serves as a key precursor in the production of caprolactam,[20] while perillartine finds extensive application in the flavor industry.[21]

Recently, researchers explored the electrocatalytic NO_x reduction coupling reaction and demonstrated the preliminary feasibility of electrocatalytic synthesis of oximes using NO_x as a nitrogen source (Fig. 1). For instance, existing literature reports that oximes such as pyridine aldoxime,[22] cyclohexa-

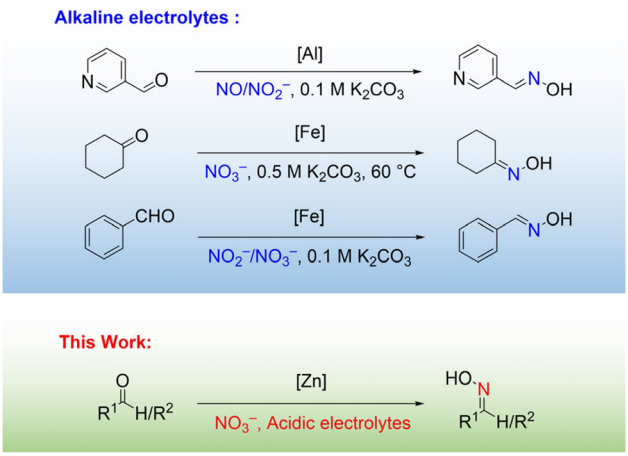

Fig. 1 Electrochemical C–N coupling of aldehydes and ketones with NO_x.

[a]*Shanghai Key Laboratory of Green Chemistry and Chemical Processes, State Key Laboratory of Petroleum Molecular & Process Engineering, School of Chemistry and Molecular Engineering, East China Normal University, Shanghai 200062, China. E-mail: sqjia@chem.ecnu.edu.cn, hhwu@chem.ecnu.edu.cn, hanbx@iccas.ac.cn*
[b]*Institute of Eco-Chongming, 20 Cuiniao Road, ChenjiaTown, Chongming District, Shanghai 202162, China*
[c]*Beijing National Laboratory for Molecular Sciences, CAS Key Laboratory of Colloid and Interface and Thermodynamics, Center for Carbon Neutral Chemistry, CAS Research/Education Center for Excellence in Molecular Sciences, Institute of Chemistry, Chinese Academy of Sciences, Beijing 100190, China*
† Electronic supplementary information (ESI) available. See DOI: https://doi.org/10.1039/d4gc03429e

none oxime,[23] and benzaldoxime[24] have been synthesized using Al-based and Fe-based catalysts with NO, NO_2^- or NO_3^- as nitrogen sources. These electrochemical coupling strategies are typically conducted under alkaline conditions because the alkaline environment restricts the electrochemical hydrogenation of substrates, thereby driving the coupling step.[25,26] However, in neutral or alkaline environments, the proton concentration is low, with most of the hydrogen in NH_2OH originating from water.[27]

Furthermore, currently available electrocatalysts are still limited, and the balance between stability and activity under alkaline conditions needs further optimization.[28–31] In view of this, there is an urgent need to develop catalytic systems for the electrocatalytic synthesis of oximes under acidic conditions. Acidic conditions offer advantages such as increased proton concentration, enhanced system stability, and potential yield improvement, aiding in overcoming limitations associated with alkaline conditions and providing new avenues and higher yields for the reaction.[32–35] Although Wu *et al.* proposed a reaction route for the synthesis of cyclohexanone by NO_2^- electrochemical reduction coupling of cyclo-hexanone under acidic conditions.[36] It is still a challenge to achieve efficient C–N coupling under acidic conditions with NO_3^- as the nitrogen source.

Herein, we report a novel electrochemical strategy for the synthesis of high value-added oximes from aldehyde/ketone and NO_3^- in an acidic electrolyte using electrodeposited modified Zn catalyst (multilayered Zn nanosheets catalyst, M-ZnNSs) as an electrode. 99% yield and 99% selectivity of phenylacetaldehyde oxime were achieved at a constant current of −12 mA cm^{-2}. The durability of the catalyst was verified by maintaining high performance after 10 cycle tests (>100 h). A series of controlled experiments, combined with *in-situ* attenuated total reflectance infrared spectroscopy (ATR-FTIR) and online differential electrochemical mass spectrometry (DEMS) tests, were conducted to elucidate the reaction pathway: NO_3^- → NH_2OH → oxime. In addition, isotope labeling experiments demonstrated that the N source was derived from NO_3^-. Importantly, this strategy exhibits broad applicability, not only for aldehydes but also for ketones. This work introduces a novel catalytic system for the value-added conversion of NO_x, with significant implications for energy and environmental sustainability.

Results and discussion

The synthesis of oximes from aldehydes and NO_3^- involves two main steps: NO_3^- reduction to $*NH_2OH$ at the electrode surface, followed by nucleophilic addition–elimination with aldehydes to form oximes and eliminate water. This process includes electrochemical (*e.g.*, hydrogenation and hydrodeoxygenation) and non-electrochemical pathways.[24] Therefore, controlling the electrochemical hydrogenation process in acidic media without affecting intermediate production rates is crucial for target product formation. It is worth mentioning that oxime is unstable in acidic conditions and may convert to other organic nitrogen compounds. This places extreme demands on both the electrode and electrolyte.

Based on the understanding of the reaction mechanism described above, we first utilized metallic materials commonly employed in electrocatalytic reactions as electrodes to directly electrosynthesize oximes, aiming to identify suitable catalysts (Fig. 2a). In the initial screening experiments, a weakly acidic buffer solution (1 M PBS, pH = 5.8) was used as the electrolyte to limit the electrochemical hydrogenation process of the organics and to ensure that the products could exist stably. Phenylacetaldehyde (PAH) and KNO_3 were used as organic compounds and NO_x model compounds, respectively, and electrolyzed at −12 mA cm^{-2} for 10 h. Although different electrode materials have different electrosynthesis oxime yields and selectivity in the co-reduction process of KNO_3 and PAH, all electrode generated products can stably exist in the electrolyte. Pt and Fe catalysts primarily drive hydrogenation reac-

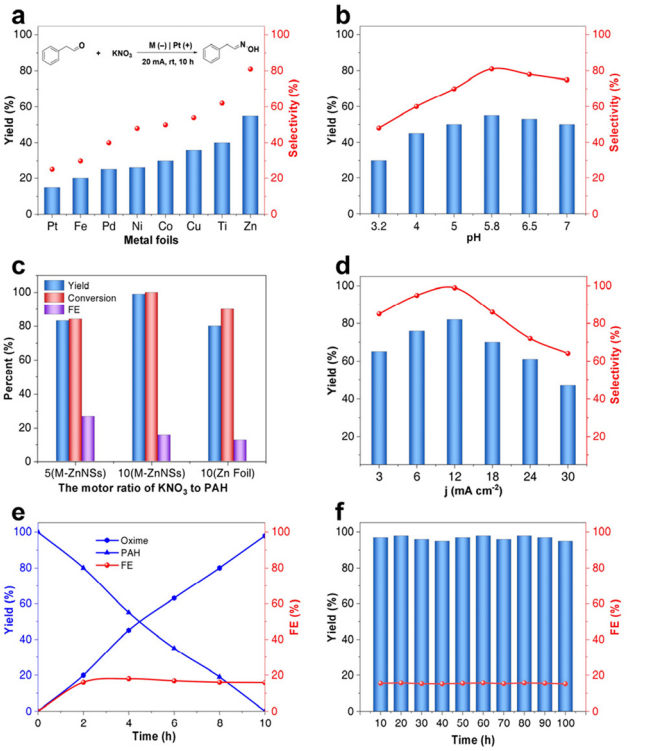

Fig. 2 Electrosynthesis of phenylacetaldehyde oxime performance from KNO_3. (a) Screening of catalysts for the electrosynthesis of phenylacetaldehyde oxime using phenylacetaldehyde and KNO_3 as feedstock. Reaction conditions: substrate (0.4 mmol), metal electrode (working area: 1.1 × 1.5 cm^2), 1 mol L^{-1} PBS containing 0.4 mol L^{-1} KNO_3 (5 mL), −12 mA cm^{-2}, 10 h. (b) Effect of different pH on the electrosynthesis of phenylacetaldehyde oxime over Zn foil. (c) Effect of different current densities for phenylacetaldehyde oxime yield and selectivity with a total 720 C of charge using M-ZnNSs electrode. (d) The effect of molar ratio of KNO_3 to PAH over different electrodes. (e) Time-dependent PAH conversion, phenylacetaldehyde oxime yield and FE using M-ZnNSs electrode. (f) The long-term stability test for phenylacetaldehyde oxime yield and FE on M-ZnNSs.

tions due to their strong reducing abilities (ESI Fig. S1†). Despite improved selectivity for oximes, catalysts like Pd, Ni, Cu, *etc*., still struggle to effectively limit hydrogenation. Encouragingly, Zn catalysts show a different selectivity, drastically reducing aldehyde hydrogenation and favoring C–N coupling to form oximes as the main reaction pathway.

We further investigated the effect of acidic electrolyte at different pH on the electrosynthesis of oximes when Zn foil was used as catalyst. The pH of the electrolyte played a decisive role in maintaining the stability of the oximes. In addition, although pH was not directly related to the non-electrochemical coupling process, it will inhibit the non-electrochemical coupling by affecting the electrochemical hydrogenation of key intermediates and the hydrodeoxygenation of aldehydes (hydride yield at different pH in ESI Fig. S2†). Acidic electrolytes with different pH were realized by preparing different buffer solutions (for detailed steps see ESI†). As shown in Fig. 2b, when the electrolyte was at medium acidity (pH = 3.2), the feedstock was dominated by the hydrogenation reaction (32% yield of alcohols), which inhibited the coupling reaction. Under strong acid conditions, there were some hydrolysis products of oxime, which also led to the decrease of the yield and selectivity of the target product. The stability of product improved as the pH was raised gradually. At pH = 5, hydrolysis of the oxime hardly happened, but some alcohol by-product was produced. Optimal selectivity and yield of oxime were achieved at pH = 5.8. However, increasing the pH further led to some side reactions in the feedstock, slightly reducing oxime selectivity.

After identifying the metal and optimal electrolyte, we proceeded to electrochemically modify commercial Zn foil, thus obtaining different modified Zn electrodes (for detailed steps see ESI†). The modified-Zn electrodes were prepared *via* a two-electrode constant-current deposition method, controlling deposition parameters such as current and time, while utilizing different Zn salt precursors and KOH concentrations to fabricate a series of Zn-based electrodes (ESI Fig. S3†). The performance of modified Zn electrodes with different Zn salts were examined by electrolysis at −12 mA cm^{-2} for 10 h, the results were shown in ESI Fig. S4.† The multilayered Zn nanosheets catalysts prepared with $ZnCl_2$ (M-ZnNSs) showed the best catalytic performance, with 99% selectivity for oxime (ESI Fig. S5 and S6†). The desired nanosheets were obtained when $ZnCl_2$ was used as the deposition solution at −90 mA cm^{-2} for 2 min. Scanning electron microscopy (SEM) revealed densely arranged layered Zn flakes on the electrode, contrasting with the smooth surface of unmodified Zn foil (ESI Fig. S7 and S8†), with an overall thickness of the nanosheets about 3 μm (ESI Fig. S9†). X-ray diffraction (XRD) analysis confirmed their highly crystalline nature, with diffraction peaks matching those of bulk Zn foil (ESI Fig. S10†). X-ray photoelectron spectroscopy (XPS) indicated Zn valence states close to 0 (ESI Fig. S11†), consistent with the zero-valence state of Zn atoms observed in X-ray absorption near-edge structure (XANES) spectra (ESI Fig. S12†).

To further improve the yield of oxime, different current densities in the range of −3 to −30 mA cm^{-2} was used for electrolysis while ensuring the passage of the same amount of charge (720 C). As shown in Fig. 2c, at lower current densities, the yield and selectivity of oxime were lower, the key intermediate $*NH_2OH$ was less and the feedstock failed to combine with it in time and other side reactions occurred. Increasing the current initially boosted oxime production, reaching a peak selectivity of 99% and yield of 82% at −12 mA cm^{-2}. Yet, further current increase led to declining yield and selectivity due to raw material instability. This triggered more self-hydrogenation, raising phenylethanol by-product levels and impeding the desired reaction (ESI Fig. S13†).

Subsequently, the performance of electrocatalytic synthesis of oximes was evaluated at different KNO_3/PAH molar ratios. As illustrated in Fig. 2d, when the molar ratio was at 5 : 1, although the selectivity of oxime was high, PAH was not completely converted, indicating that the $*NH_2OH$ produced during the KNO_3 reduction process was not sufficient to completely convert the PAH into oxime. Increasing the molar ratio to 10 : 1, all PAH in the system was basically converted to oxime. To show the superiority of the electrochemically modified Zn foil strategy, we used unmodified Zn foil for the electrosynthesis of oximes at the optimum molar ratio, and its performance was not as good as that of M-ZnNSs. To further enhance the yield and selectivity of electrochemically synthesizing oxime, we also investigated the effect of reaction time. As shown in Fig. 2e, the optimal reaction time was 10 h, PAH was completely converted into oxime. Moreover, the durability of the electrocatalyst was also evaluated (Fig. 2f). After 10 consecutive electrical cycles (about 100 h), there was no obvious decrease in the yield and selectivity of oximes, which demonstrated the excellent stability of the M-ZnNSs catalysts and proved their excellent recyclability, which is important for practical applications. Moreover, the crystallographic structure, and compositions of M-ZnNSs electrode remained stable even after 100 h of reaction (ESI Fig. S14†).

To gain a deeper understanding of the reaction pathways and excellent performance of M-ZnNSs electrocatalysts, a series of mechanistic experiments were conducted. The C–N coupling reactions were carried out using $K^{14}NO_3$ and $K^{15}NO_3$ as nitrogen sources to reveal the source of nitrogen in the resulting oximes (Fig. 3a and b). A molecular ion peak of 136 appears in the $K^{15}NO_3$ solution, while the $K^{14}NO_3$ system shows a molecular ion peak of 135, demonstrating that the nitrogen in the coupling product is derived from nitrate. In addition, *in-situ* ATR-FTIR spectroscopy was used to gain insight into the reaction pathway of C–N coupling on M-ZnNSs electrocatalysts. As shown in Fig. 3c, with the increase of electrolysis time, the M-ZnNSs showed IR absorption peaks at 1632 cm^{-1}, which may be the characteristic peak of NH_2OH.[37] The persistence of this absorption peak indicates that NH_2OH is stable during the electrolysis process. To further verify that NH_2OH intermediates were produced during the reaction process, an online DEMS was used to analyze the reaction with optimal reaction conditions. As shown in Fig. 3d, applying the current, the mass spectral signal of NH_2OH could be detected, which proved that NH_2OH was produced during the reduction

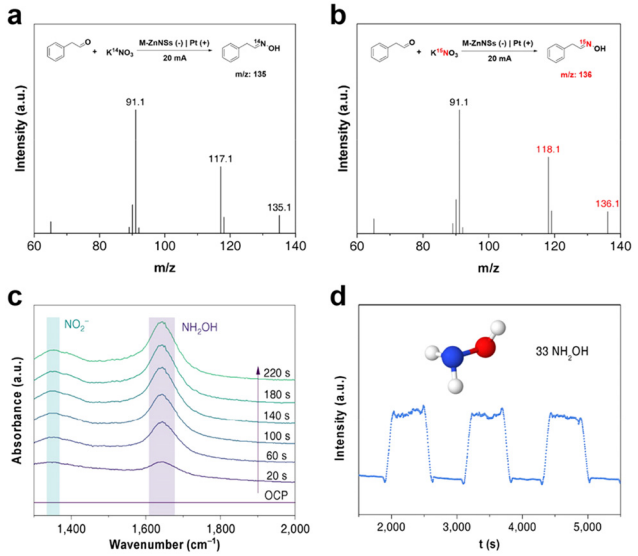

Fig. 3 Reaction mechanism investigation. (a) The mass-spectrometry spectrum of the electrocatalytic synthesis of phenylacetaldehyde oxime from $K^{14}NO_3$ and PAH. (b) The mass-spectrometry spectrum of the electrocatalytic synthesis of phenylacetaldehyde oxime from $K^{15}NO_3$ and PAH. (c) Time-gradient electrolysis test using *in-situ* ATR-FTIR on M-ZnNSs under working condition. (d) Online DEMS measurements for the NO_3RR over the M-ZnNSs electrode.

of KNO_3 (other nitrogen-containing products were shown in ESI Fig. S15†).

To demonstrate the versatility of this catalytic system, we carried out electrosynthesis of various oximes bearing substituent groups over the M-ZnNSs electrode, such as aldehyde oxime and ketone oxime (as shown in Fig. 4 and ESI Fig. S16–27†). It is shown that this method was applicable to synthesizing different types of aldehyde oximes in high yields (yield and selectivity >90%), demonstrating the high versatility of this method. The above results indicate that the electrochemical *in-situ* production of hydroxylamine offers high feasibility for converting nitrogen-containing waste gases and wastewater into high-value organic nitrogen compounds.

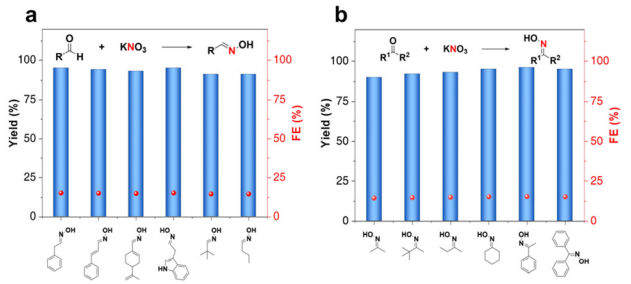

Fig. 4 Substrate expansion and universality studies. (a) Reaction scope of the direct electrosynthesis of aldehyde oxime from KNO_3 and R-CHO. Reaction conditions: RCHO (40 mM), M-ZnNSs (working area: 1.1 × 1.5 cm^2), 1 mol L^{-1} PBS containing 0.4 mol L^{-1} KNO_3 (5 mL), –12 mA cm^{-2}, 10 h, isolated yield. (b) Reaction scope of the direct electrosynthesis of ketone oxime from KNO_3 and ketone. Reaction conditions: R_1COR_2 (40 mM), M-ZnNSs (working area: 1.1 × 1.5 cm^2), 1 mol L^{-1} PBS containing 0.4 mol L^{-1} KNO_3 (5 mL), –12 mA cm^{-2}, 10 h, isolated yield.

Conclusions

In conclusion, we present a novel catalytic system for the synthesis of oximes using NH_2OH generated by KNO_3 electrocatalytic reduction coupled with aldehyde/ketone compounds under acidic conditions over Zn-based catalysts. The catalytic system achieved outstanding results in oxime electrosynthesis, offering high yield, selectivity, broad substrate compatibility, functional group tolerance, and long-term stability. It also excelled in synthesizing cinnamaldehyde oximes for food flavors and butyl ketones oximes for coating antioxidants. This study not only lays the groundwork for designing efficient catalytic systems for C–N coupling, enabling the conversion of nitrates into valuable oximes, but also expands efficient NH_2OH production methods with promising applications.

Author contributions

C. X., S. Q. J., H. H. W. and B. X. H. proposed the project, designed the experiments, and wrote the manuscript. C. X. performed the whole experiments. J. P. J., X. C., Z. H. X., M. K. D., T. D., H. L. C. and C. J. C. performed the analysis of experimental data. S. Q. J., H. H. W., M. Y. H. and B. X. H. co-supervised the whole project. All authors discussed the results and commented on the manuscript.

Data availability

All data generated or analyzed in this study are included in this manuscript and ESI.† The datasets used and/or analyzed in this study are available upon request from the corresponding authors. The data are available in the publicly available in a public repository.

Conflicts of interest

The authors declare no competing interests.

Acknowledgements

The work was supported by the National Key R&D Program of China (2023YFA1507901, 2020YFA0710201), the National Natural Science Foundation of China (22293015, 22121002), the China Postdoctoral Science Foundation (2023M731096), and the Fundamental Research Funds for the Central Universities.

References

1 C. J. Stevens, *Science*, 2019, **363**, 578–580.
2 O. S. G. P. Soares, J. J. M. Órfão, J. Ruiz-Martínez, J. Silvestre-Albero, A. Sepúlveda-Escribano and M. F. R. Pereir, *Chem. Eng. J.*, 2010, **165**, 78–88.
3 J. Li, X. Han, X. Zhang, A. M. Sheveleva, Y. Cheng, F. Tuna, E. J. L. McInnes, L. J. M. McPherson, S. J. Teat, L. L. Daemen, A. J. Ramirez-Cuesta, M. Schröder and S. Yang, *Nat. Chem.*, 2019, **11**, 1085–1090.
4 C. Mao, J. Wang, Y. Zou, Y. Shi, C. J. Viasus, J. Y. Y. Loh, M. Xia, S. Ji, M. Li, H. Shang, M. Ghoussoub, Y.-F. Xu, J. Ye, Z. Li, N. P. Kherani, L. Zheng, Y. Liu, L. Zhang and G. A. Ozin, *J. Am. Chem. Soc.*, 2023, **145**, 13134–13146.
5 M. Wu, J. Li, A. O. Leu, D. V. Erler, Z. Yuan, S. J. McIlroy, T. Stark, G. W. Tyson and J. Guo, *Nat. Commun.*, 2022, **13**, 6115.
6 K. Liu, H. Li, M. Xie, P. Wang, Z. Jin, Y. Liu, M. Zhou, P. Li and G. Yu, *J. Am. Chem. Soc.*, 2024, **146**, 7779–7790.
7 D. Xu, Y. Li, L. Yin, Y. Ji, J. Niu and Y. Yu, *Front. Environ. Sci. Eng.*, 2018, **12**, 1–14.
8 Y. Cheng, S. Liu, J. Jiao, M. Zhou, Y. Wang, X. Xing, Z. Chen, X. Sun, Q. Zhu, Q. Qian, C. Wang, H. Liu, Z. Liu, X. Kang and B. Han, *J. Am. Chem. Soc.*, 2024, **46**, 10084–10092.
9 M. He, Y. Wu, R. Li and B. Zhang, *Nat. Commun.*, 2023, **14**, 5088.
10 S. Jia, L. Wu, H. Liu, R. Wang, X. Sun and B. Han, *Angew. Chem., Int. Ed.*, 2024, **63**, e202400033.
11 M. Li, Y. Wu, B.-H. Zhao, C. Cheng, J. Zhao, C. Liu and B. Zhang, *Nat. Catal.*, 2023, **6**, 906–915.
12 J. Wu, L. Xu, Z. Kong, K. Gu, Y. Lu, X. Wu, Y. Zou and S. Wang, *Angew. Chem., Int. Ed.*, 2023, **62**, e202311196.
13 Y. Wu, Z. Jiang, Z. Lin, Y. Liang and H. Wang, *Nat. Sustainability*, 2021, **4**, 725–730.
14 Y. Wu, M. Li, T. Li, J. Zhao, Z. Song and B. Zhang, *Sci. China: Chem.*, 2023, **66**, 1854–1859.
15 J. Xian, S. Li, H. Su, P. Liao, S. Wang, R. Xiang, Y. Zhang, Q. Liu and G. Li, *Angew. Chem., Int. Ed.*, 2023, **62**, e202306726.
16 J. Xian, S. Li, H. Su, P. Liao, S. Wang, Y. Zhang, W. Yang, J. Yang, Y. Sun, Y. Jia, Q. Liu, Q. Liu and G. Li, *Angew. Chem., Int. Ed.*, 2023, **62**, e202304007.
17 D. S. Bolotin, N. A. Bokach, M. Y. Demakova and V. Y. Kukushkin, *Chem. Rev.*, 2017, **117**, 13039–13122.
18 S. Ji, L. Zhao, B. Miao, M. Xue, T. Pan, Z. Shao, X. Zhou, A. Fu and Y. Zhang, *Angew. Chem., Int. Ed.*, 2023, **62**, e202304434.
19 W. Xue, Y. Jiang, H. Lu, B. You, X. Wang and C. Tang, *Angew. Chem., Int. Ed.*, 2023, **62**, e202314364.
20 R. J. Lewis, K. Ueura, X. Liu, Y. Fukuta, T. E. Davies, D. J. Morgan, L. Chen, J. Qi, J. Singleton, J. K. Edwards, S. J. Freakley, C. J. Kiely, Y. Yamamoto and G. J. Hutchings, *Science*, 2022, **376**, 615–620.
21 M. S.-N. Gabriela Juárez, J. L. Alonso, E. R. Alonso and I. León, *Molecules*, 2022, **27**, 1924.
22 R. Xiang, S. Wang, P. Liao, F. Xie, J. Kang, S. Li, J. Xian, L. Guo and G. Li, *Angew. Chem., Int. Ed.*, 2023, **62**, e202312239.
23 Y. Wu, W. Chen, Y. Jiang, Y. Xu, B. Zhou, L. Xu, C. Xie, M. Yang, M. Qiu, D. Wang, Q. Liu, Q. Liu, S. Wang and Y. Zou, *Angew. Chem., Int. Ed.*, 2023, **62**, e202305491.
24 W. Chen, Y. Wu, Y. Jiang, G. Yang, Y. Li, L. Xu, M. Yang, B. Wu, Y. Pan, Y. Xu, Q. Liu, C. Chen, F. Peng, S. Wang and Y. Zou, *J. Am. Chem. Soc.*, 2024, **146**, 6294–6306.
25 D. C. Cantu, A. B. Padmaperuma, M.-T. Nguyen, S. A. Akhade, Y. Yoon, Y.-G. Wang, M.-S. Lee, V.-A. Glezakou, R. Rousseau and M. A. Lilga, *ACS Catal.*, 2018, **8**, 7645–7658.
26 X. H. Chadderdon, D. J. Chadderdon, J. E. Matthiesen, Y. Qiu, J. M. Carraher, J.-P. Tessonnier and W. Li, *J. Am. Chem. Soc.*, 2017, **139**, 14120–14128.
27 G. Zhang, X. Li, K. Chen, Y. Guo, D. Ma and K. Chu, *Angew. Chem., Int. Ed.*, 2023, **62**, e202300054.
28 M. S. Burke, M. G. Kast, L. Trotochaud, A. M. Smith and S. W. Boettcher, *J. Am. Chem. Soc.*, 2015, **137**, 3638–3648.
29 E. Fabbri, M. Nachtegaal, T. Binninger, X. Cheng, B.-J. Kim, J. Durst, F. Bozza, T. Graule, R. Schäublin, L. Wiles, M. Pertoso, N. Danilovic, K. E. Ayers and T. J. Schmidt, *Nat. Mater.*, 2017, **16**, 925–931.
30 L. Han, S. Dong and E. Wang, *Adv. Mater.*, 2016, **28**, 9266–9291.
31 X. Zou and Y. Zhang, *Chem. Soc. Rev.*, 2015, **44**, 5148.
32 Y. Guo, R. Zhang, S. Zhang, Y. Zhao, Q. Yang, Z. Huang, B. Dong and C. Zhi, *Energy Environ. Sci.*, 2021, **14**, 3938–3944.
33 J. Yu, Y. Qin, X. Wang, H. Zheng, K. Gao, H. Yang, L. Xie, Q. Hu and C. He, *Nano Energy*, 2022, **103**, 107705.
34 R. Zhang, C. Li, H. Cui, Y. Wang, S. Zhang, P. Li, Y. Hou, Y. Guo and C. Zhi, *Nat. Commun.*, 2023, **14**, 8036.
35 Y. Zheng, Y. Jiao, A. Vasileff and S.-Z. Qiao, *Angew. Chem., Int. Ed.*, 2018, **57**, 7568–7579.
36 Y. Wu, B.-H. Zhao, Z. Song, C. Liu, J. Zhao, C. Wang, T. Li and B. Zhang, *Nat. Commun.*, 2023, **14**, 3057.
37 R. Hao, S. Fang, L. Tian, R. Xia, Q. Guan, L. Jiao, Y. Liu and W. Li, *Chem. Eng. J.*, 2023, **467**, 143371.